Chapter 4

Results

In this chapter, we first give the results of SIR-PDE models. Then we show the results of conversion of an SIR-PDE model to an SIR-CA model for von Neumann neighborhood. Next, we give the results of the simulation for SIR-CA model with two neighborhoods, von Neumann and Moore. After that, we show the results of the comparison between the discretized SIR-PDE model and SIR-CA model. Finally, we show the SIS model that is created by cellular automata and give the results of the computer program to simulate an SIS-CA model.

4.1 Creation of a reaction-diffusion PDE model for SIR-type epidemics.

We will develop a reaction-diffusion PDE model for SIR-type epidemics. We assume that the population densities of susceptible *S*, infected *I* and recovered *R* populations are functions of space variables *x,y* and time *t*. The populations can change by diffusion from regions of higher concentration to regions of lower concentration with the same diffusion coefficient *k*. We assume that the people in the *S* population can become infected when they come into contact with infected people in the *I* population at the same position at the same time. The model is of the form:

$$\begin{aligned} \frac{\partial S}{\partial t} &= k\nabla^2 S - \alpha SI \\ \frac{\partial I}{\partial t} &= k\nabla^2 I + \alpha SI - \beta I \qquad (4\text{-}1) \\ \frac{\partial R}{\partial t} &= k\nabla^2 R + \beta I \end{aligned}$$

where k is a diffusion coefficient

α is an infection rate of susceptible individuals

β is a recovery rate of infected individual

We also assume that the total population density $N = S + I + R$ is initially independent of position, i.e., $\nabla^2 N = 0$ at $t = 0$. Then Eq. (4-1) give that $\frac{\partial N}{\partial t} = k\nabla^2 N = 0$ at $t = 0$ and therefore N is independent of position and time.

The terms in this model are different from the SIR-PDE model in Eq. (3-1) because our assumptions are different. In Eq. (3-1), the people are assumed to remain at the same position and infection is assumed to occur through a non-local interaction between a susceptible individual at one position and infected individuals in neighboring positions. In the reaction-diffusion model, the people are assumed to move in space by a diffusion process and the infection is assumed to occur through a local interaction between infected and susceptible people at the same position in space.

We use discretization to convert the SIR-PDE model to SIR-CA model for von Neumann neighborhood in the next section.

4.2 The Results of Conversion of SIR-PDE Model to SIR-CA Model for von Neumann Neighborhood

After applying the discretization method to Eq. (4-1), we obtain the discretized model:

$$\begin{aligned}
\frac{S_{i,j}^{n+1} - S_{i,j}^{n}}{\Delta t} &= k\left(\frac{S_{i+1,j}^{n} - 2S_{i,j}^{n} + S_{i-1,j}^{n}}{(\Delta x)^2} + \frac{S_{i,j+1}^{n} - 2S_{i,j}^{n} + S_{i,j-1}^{n}}{(\Delta y)^2}\right) - \alpha S_{i,j}^{n} I_{i,j}^{n}, \\
\frac{I_{i,j}^{n+1} - I_{i,j}^{n}}{\Delta t} &= k\left(\frac{I_{i+1,j}^{n} - 2I_{i,j}^{n} + I_{i-1,j}^{n}}{(\Delta x)^2} + \frac{I_{i,j+1}^{n} - 2I_{i,j}^{n} + I_{i,j-1}^{n}}{(\Delta y)^2}\right) + \alpha S_{i,j}^{n} I_{i,j}^{n} - \beta I_{i,j}^{n}, \qquad (4\text{-}2) \\
\frac{R_{i,j}^{n+1} - R_{i,j}^{n}}{\Delta t} &= k\left(\frac{R_{i+1,j}^{n} - 2R_{i,j}^{n} + R_{i-1,j}^{n}}{(\Delta x)^2} + \frac{R_{i,j+1}^{n} - 2R_{i,j}^{n} + R_{i,j-1}^{n}}{(\Delta y)^2}\right) + \beta I_{i,j}^{n}.
\end{aligned}$$

Assuming a lattice of square cells of side ε, we let $\Delta x = \Delta y = \varepsilon$ and then Eq. (4-2) becomes

$$\begin{aligned}
\frac{S_{i,j}^{n+1}-S_{i,j}^{n}}{\Delta t} &= k\left(\frac{S_{i+1,j}^{n}-2S_{i,j}^{n}+S_{i-1,j}^{n}}{\varepsilon^2}+\frac{S_{i,j+1}^{n}-2S_{i,j}^{n}+S_{i,j-1}^{n}}{\varepsilon^2}\right)-\alpha S_{i,j}^{n}I_{i,j}^{n},\\
\frac{I_{i,j}^{n+1}-I_{i,j}^{n}}{\Delta t} &= k\left(\frac{I_{i+1,j}^{n}-2I_{i,j}^{n}+I_{i-1,j}^{n}}{\varepsilon^2}+\frac{I_{i,j+1}^{n}-2I_{i,j}^{n}+I_{i,j-1}^{n}}{\varepsilon^2}\right)+\alpha S_{i,j}^{n}I_{i,j}^{n}-\beta I_{i,j}^{n},\\
\frac{R_{i,j}^{n+1}-R_{i,j}^{n}}{\Delta t} &= k\left(\frac{R_{i+1,j}^{n}-2R_{i,j}^{n}+R_{i-1,j}^{n}}{\varepsilon^2}+\frac{R_{i,j+1}^{n}-2R_{i,j}^{n}+R_{i,j-1}^{n}}{\varepsilon^2}\right)+\beta I_{i,j}^{n}.
\end{aligned} \tag{4-3}$$

If we number the cells in the lattice as (i, j) and let n be a counter for time steps, we obtain the model shown below:

$$\begin{aligned}
S_{i,j}^{n+1} &= (1-\frac{4k\Delta t}{\varepsilon^2})S_{i,j}^{n}+\frac{k\Delta t}{\varepsilon^2}\left(S_{i+1,j}^{n}+S_{i-1,j}^{n}+S_{i,j+1}^{n}+S_{i,j-1}^{n}\right)-\alpha\Delta t S_{i,j}^{n}I_{i,j}^{n},\\
I_{i,j}^{n+1} &= (1-\frac{4k\Delta t}{\varepsilon^2}-\beta\Delta t)I_{i,j}^{n}+\frac{k\Delta t}{\varepsilon^2}\left(I_{i+1,j}^{n}+I_{i-1,j}^{n}+I_{i,j+1}^{n}+I_{i,j-1}^{n}\right)+\alpha\Delta t S_{i,j}^{n}I_{i,j}^{n},\\
R_{i,j}^{n+1} &= (1-\frac{4k\Delta t}{\varepsilon^2})R_{i,j}^{n}+\frac{k\Delta t}{\varepsilon^2}\left(R_{i+1,j}^{n}+R_{i-1,j}^{n}+R_{i,j+1}^{n}+R_{i,j-1}^{n}\right)+\beta\Delta t I_{i,j}^{n}.
\end{aligned} \tag{4-4}$$

It can be seen from Eq. (4-4) that the CA equations will only give an acceptable non-negative solution if $4k\frac{\Delta t}{\varepsilon^2}+\beta\Delta t<1$. If we choose a time step and cell size of $\Delta t=\varepsilon=1$, Eq. (4-4) reduces to Eq. (4-5)

$$\begin{aligned}
S_{ij}^{n+1} &= (1-4k)S_{ij}^{n}+k\left(S_{i+1,j}^{n}+S_{i-1,j}^{n}+S_{i,j+1}^{n}+S_{i,j-1}^{n}\right)-\alpha S_{ij}^{n}I_{ij}^{n},\\
I_{ij}^{n+1} &= (1-4k-\beta)I_{ij}^{n}+k\left(I_{i+1,j}^{n}+I_{i-1,j}^{n}+I_{i,j+1}^{n}+I_{i,j-1}^{n}\right)+\alpha S_{ij}^{n}I_{ij}^{n},\\
R_{ij}^{n+1} &= (1-4k)R_{ij}^{n}+k\left(R_{i+1,j}^{n}+R_{i-1,j}^{n}+R_{i,j+1}^{n}+R_{i,j-1}^{n}\right)+\beta I_{ij}^{n}.
\end{aligned} \tag{4-5}$$

Eq. (4-5) represents a CA model. To obtain an acceptable non-negative solution it is necessary that $4k+\beta<1$. Using the index set W^* of the von Neumann neighborhood

$$W^*=\{(1,0),(-1,0),(0,1)(0,-1)\}. \tag{4-6}$$

We can write the transition function of SIR-CA model as follows:

$$\begin{aligned}
S_{ij}^{t+1} &= (1-4k)S_{ij}^{t}+k\sum_{(k,l)\in W^*}S_{i+k,j+l}^{t}-\alpha S_{ij}^{t}I_{ij}^{t},\\
I_{ij}^{t+1} &= (1-4k-\beta)I_{ij}^{t}+k\sum_{(k,l)\in W^*}I_{i+k,j+l}^{t}+\alpha S_{ij}^{t}I_{ij}^{t},\\
R_{ij}^{t+1} &= (1-4k)R_{ij}^{t}+k\sum_{(k,l)\in W^*}R_{i+k,j+l}^{t}+\beta I_{ij}^{t}.
\end{aligned} \tag{4-7}$$

If we use the Moore neighborhood for the CA, the approximation for the Laplacian is changed (see Appendix A) and the CA model becomes

$$\begin{aligned} S_{ij}^{t+1} &= (1-\frac{8}{3}k)S_{ij}^{t} + \frac{k}{3}\sum_{(k,l)\in W^*} S_{i+k,j+l}^{t} - \alpha S_{ij}^{t} I_{ij}^{t}, \\ I_{ij}^{t+1} &= (1-\frac{8}{3}k-\beta)I_{ij}^{t} + \frac{k}{3}\sum_{(k,l)\in W^*} I_{i+k,j+l}^{t} + \alpha S_{ij}^{t} I_{ij}^{t}, \\ R_{ij}^{t+1} &= (1-\frac{8}{3}k)R_{ij}^{t} + \frac{k}{3}\sum_{(k,l)\in W^*} R_{i+k,j+l}^{t} + \beta I_{ij}^{t}, \end{aligned} \tag{4-8}$$

where W^* is now the index set of the Moore neighborhood given by

$$W^* = \{(0,1),(0,-1),(1,0),(-1,0),(-1,-1),(-1,1),(1,-1),(1,1)\}. \tag{4-9}$$

To obtain an acceptable non-negative solution for Eq. (4-8), it is necessary that $\frac{8k}{3} + \beta < 1$. The simulation of the SIR-CA models is shown in the next section.

4.3 The Simulation of the SIR-CA Model

In this section, we show the result of simulations for three SIR-CA models. The first model follows the model of White et al [1], the second model represents the SIR-CA model in Eq. (3-5) and the third model represents the reaction-diffusion CA models in Eq. (4-7) and (4-8).

The lattice L in the three simulations is defined as a two-dimensional lattice of 50×50 square cells. We used the gray scale to represent the state of infection, from black color for state 0 to white color for state 1. The infected cells have a gray or white color. The cells that are not infected have a black color. Therefore the people in the black cell can be susceptible or recovered individuals. Suppose that the population N in each cell is equal to 100. The infection starts in the middle cell, namely $(25,25)$ with 0.3 of the population infected and 0.7 of the population susceptible. Then the start state is $s_{25,25}^{0} = (0.7, 0.3, 0)$ and all other cells are in the state (1,0,0). We chose the artificial parameters used in White et al [1] to simulate our program with the two neighborhoods. The results are shown for the six times t = 0, 5, 10, 15, 20, 25.

For the first model, the infection rate α is set equal to 0.6, recovery rate β is equal to 0.4, connection factor $c_{kl}^{(i,j)}$ for every cell is equal to 1 and movement factor $m_{kl}^{(i,j)}$ for every cell is equal to 0.5. The result for a von Neumann neighborhood is shown in FIGURE 4-1 and the result for a Moore neighborhood is shown in FIGURE (4-2). The evolutions of the numbers of susceptible, infected and recovered individuals are shown in FIGURE (4-3).

For the second model, the infection rate α is set equal to 1.8, recovery rate β is equal to 0.4, infection rate between the main cell and neighbor cell γ is equal to 0.3. The result for von Neumann neighborhood is shown in FIGURE (4-4) and the result for Moore neighborhood is shown in FIGURE (4-5). The evolutions of the numbers of susceptible, infected and recovered individuals are shown in FIGURE (4-6).

For the third model, an infection rate α is set equal to 0.7, recovery rate β is equal to 0.3, movement rate k are equal to 0.05. The result for von Neumann neighborhood is shown in FIGURE (4-7) and the result for Moore neighborhood is shown in FIGURE (4-8). The evolutions of the number of susceptible, infected and recovered individuals are shown in FIGURE (4-9).

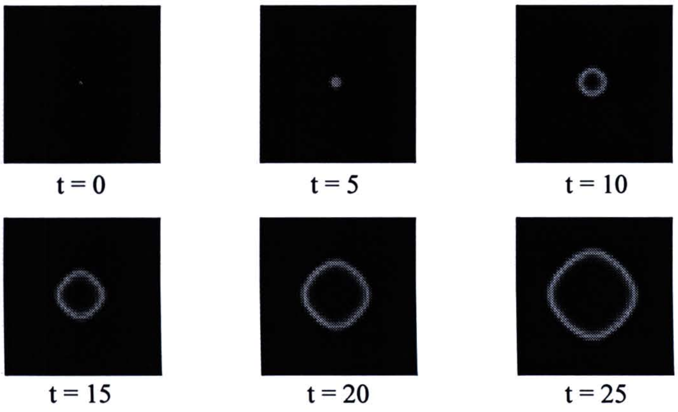

FIGURE 4-1 Simulation of the first SIR-CA model for von Neumann neighborhood

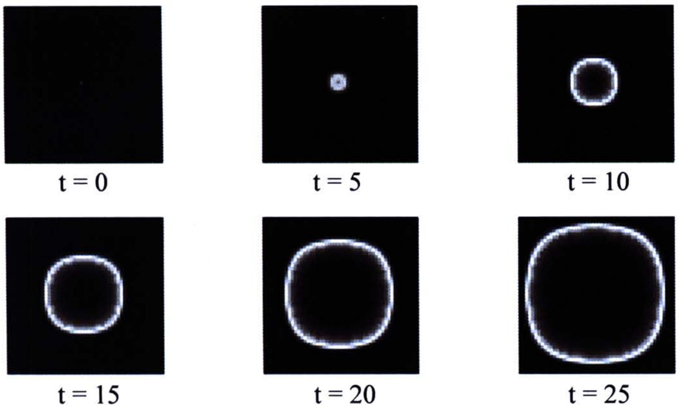

t = 0 t = 5 t = 10

t = 15 t = 20 t = 25

FIGURE 4-2 Simulation of the first SIR-CA model for Moore neighborhood

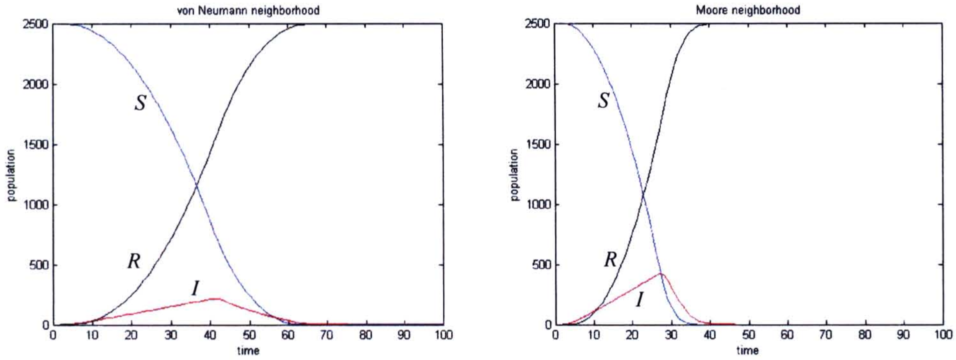

FIGURE 4-3 Evolution of the numbers of susceptible, infected and recovered individuals in the first SIR-CA model

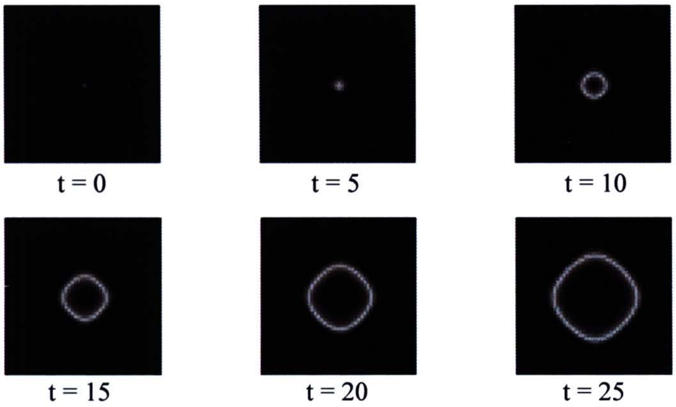

t = 0 t = 5 t = 10

t = 15 t = 20 t = 25

FIGURE 4-4 Simulation of the second SIR-CA model for von Neumann neighborhood

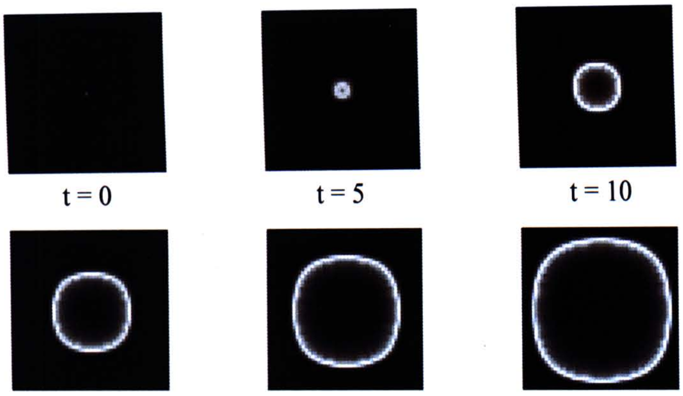

t = 0 t = 5 t = 10

t = 15 t = 20 t = 25

FIGURE 4-5 Simulation of the second SIR-CA model for Moore neighborhood

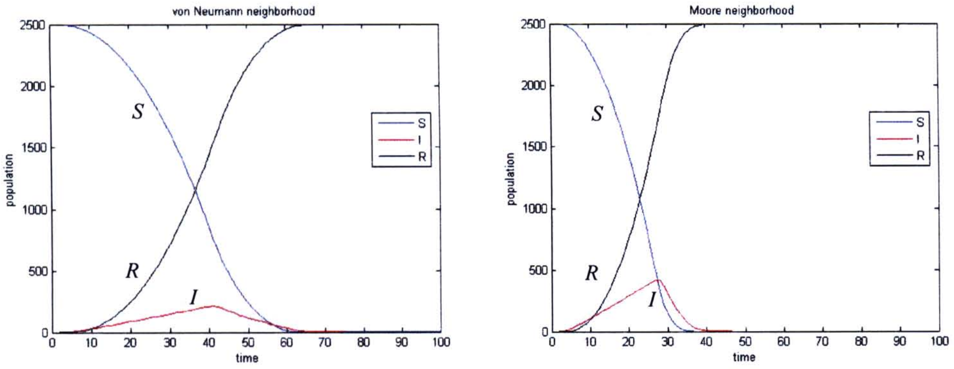

FIGURE 4-6 Evolution of the numbers of susceptible, infected and recovered individuals in the second SIR-CA model

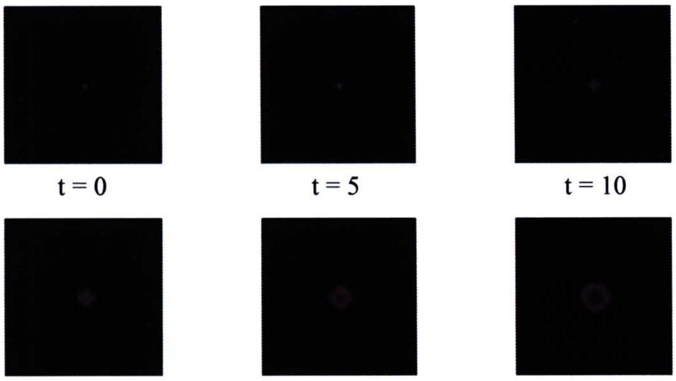

t = 0 t = 5 t = 10

t = 15 t = 20 t = 25

FIGURE 4-7 Simulation of the third SIR-CA model for von Neumann neighborhood

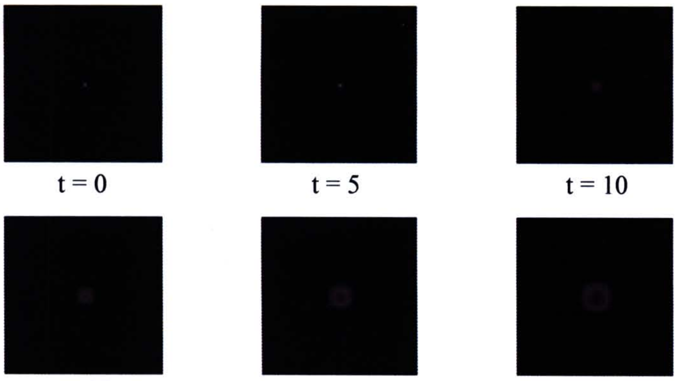

t = 0 t = 5 t = 10

t = 15 t = 20 t = 25

FIGURE 4-8 Simulation of the third SIR-CA model for Moore neighborhood

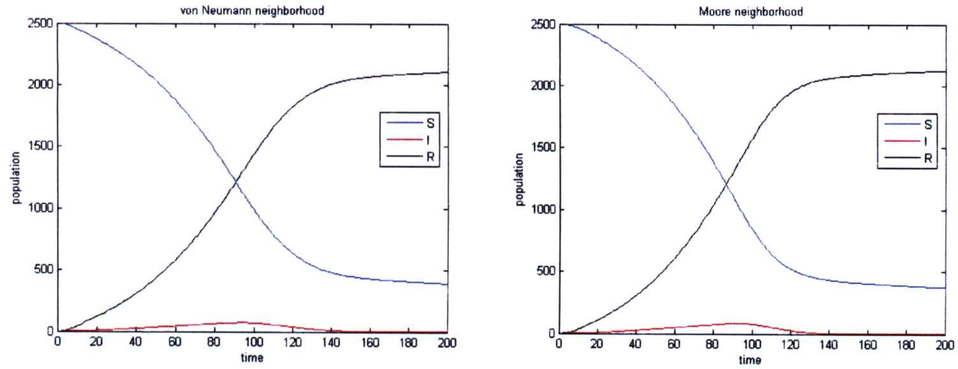

FIGURE 4-9 Evolutions of the number of susceptible, infected and recovered individuals in the reaction-diffusion SIR-CA model

The plots shown in FIGURE (4-3), FIGURE (4-6) and FIGURE (4-9) give a comparison of the evolution of the epidemic with the von Neumann and Moore neighborhoods. It can be seen that the infection in the Moore neighborhood spreads faster than in the von Neumann neighborhood because in the von Neumann neighborhood four neighbors can be infected each time step whereas in the Moore neighborhood 8 neighbors can be infected each time step.

4.4 A Comparison of Spreading Out in the Discretized SIR-PDE Model and the SIR-CA Model for von Neumann Neighborhood

We compare the result of the discretized SIR-PDE model in (4.4) with the result of the SIR-CA model in (4.7) for von Neumann neighborhood. We choose an infection rate α equal to 0.7, recovery rate β equal to 0.3, and diffusion coefficient k

for the *S*, *I* and *R* populations equal to 0.05. We compare the spreading of the epidemic for a cell size of 0.5 and time step 0.5 with a cell size and time step of 1. The PDE result corresponds to a limiting value of cell size and time step equal to 0.

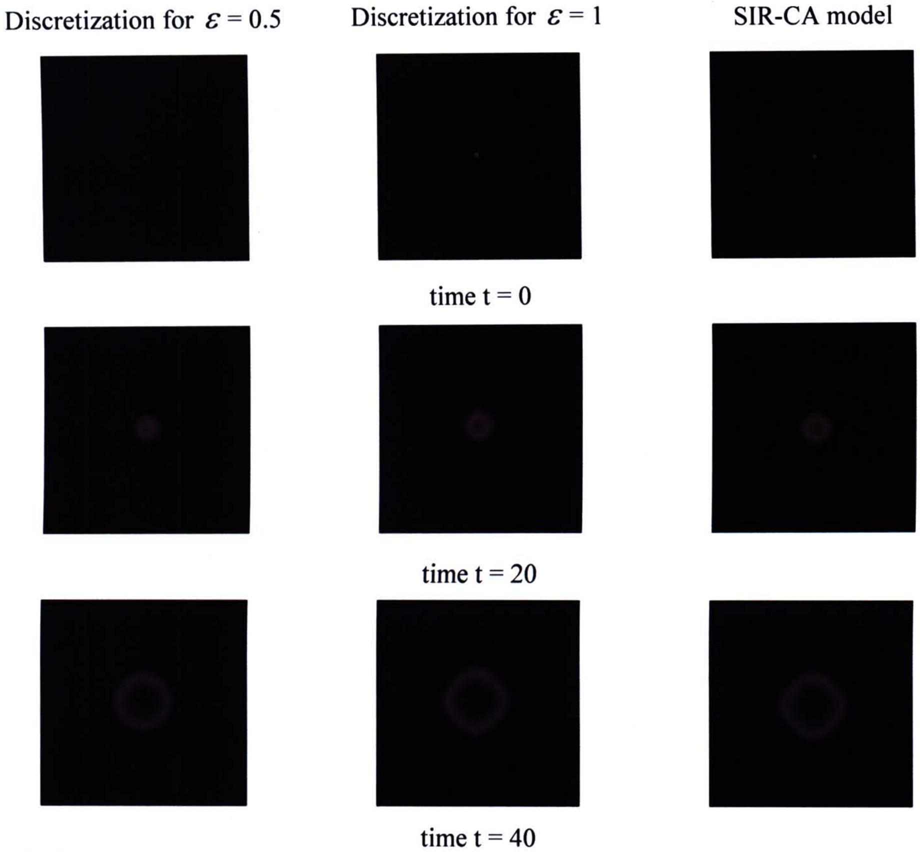

FIGURE 4-10 Comparison of the simulation between discretization of SIR-PDE model and SIR-CA model for von Neumann neighborhood

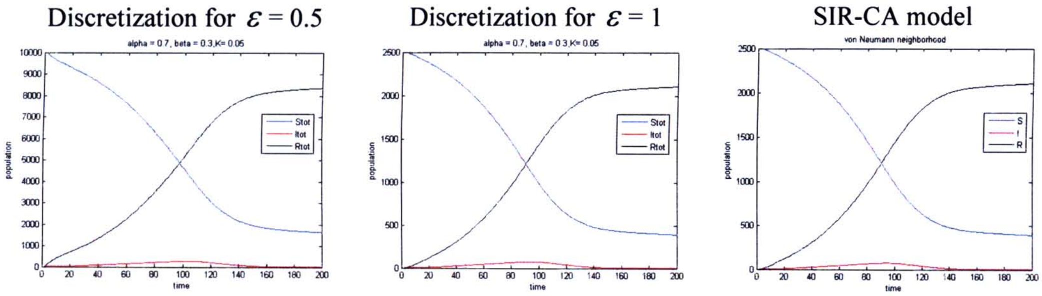

FIGURE 4-11 Comparison of the evolutions of susceptible, infected and recovered individuals in discretization of SIR-PDE model and SIR-CA model for von Neumann neighborhood

It can be seen that the qualitative behaviors of the solutions, i.e., the shapes of the population curves for the step sizes of 0.5 and 1 and for the CA-model are similar. The populations of each individual converge to steady state solutions without oscillation. The qualitative behavior of the solutions is similar, although the details are different. However, it should be noted that the behaviors will only be similar if the conditions of the form $4k+\beta<1$ required for convergence of the CA model derived from PDE are satisfied.

4.5 SIS-CA Model

We derive a CA model for an SIS-type epidemic by modifying the SIR-CA model of White et al [1]. A cellular automata model for an SIS-type epidemic consists of four parts: (1) lattice L (the ground where an epidemic is spreading out), (2) set of states Q, (3) transition function and (4) neighborhood. The composition of the SIS-CA model is the following:

- The lattice consists of square cells and the lattice size is $a \times b$.
- The set of states is $Q = K \times K$ where

  $$K \in \{0.00, 0.01, 0.02, 0.03, \ldots, 0.99, 1.00\}, \tag{4-10}$$

  and the states of cell (i,j) at time t are given in equation (4-11)

  $$s_{i,j}^{t} = \left(S_{i,j}^{t}, I_{i,j}^{t}\right). \tag{4-11}$$

  where $s_{i,j}^{t} \in Q$
- The local transition function used is the following:

  $$S_{i,j}^{t+1} = S_{i,j}^{t} - \alpha S_{i,j}^{t} I_{i,j}^{t} + \beta I_{i,j}^{t} - \alpha S_{i,j}^{t} \sum_{(k,l)\in W^{*}} c_{k,l}^{(i,j)} m_{k,l}^{(i,j)} I_{i+k,j+l}^{t}, \tag{4-12}$$

  $$I_{i,j}^{t+1} = (1-\beta) I_{i,j}^{t} + \alpha S_{i,j}^{t} I_{i,j}^{t} + \alpha S_{i,j}^{t} \sum_{(k,l)\in W^{*}} c_{k,l}^{(i,j)} m_{k,l}^{(i,j)} I_{i+k,j+l}^{t}, \tag{4-13}$$

  where W^{*} is an index set of the neighborhood.

  $c_{k,l}^{(i,j)}$ are the connection factors. In this work, we use the same three ways of transport between the cells as in White et al [1]: namely, by airplane, by train and by car or bus. This connection is given by the coefficients $c_{k,l}^{(i,j)}$ such that:

$$c_{k,l}^{(i,j)} = \begin{cases} \mathit{1}, & \text{if there exist three ways of transport between the cells,} \\ \mathit{0.6}, & \text{if there are two ways of transport between the cells,} \\ \mathit{0.3}, & \text{if there is only one way of transport between the cells,} \\ \mathit{0}, & \text{if there is no way of transport between the cells} \end{cases}$$

$m_{k,l}^{(i,j)}$ are the movement factors between the main cell (*i,j*) and its neighbor cells $(i+k, j+l)$,

α is an infection rate.

β is a recovery rate.

- The two neighborhoods used in this model are von Neumann neighborhood and Moore neighborhood. The index set of the two neighborhoods are the following:

  For von Neumann neighborhood:

  $$W^* = \{(0,1),(0,-1),(1,0),(-1,0)\}, \tag{4-14}$$

  and for Moore neighborhood:

  $$W^* = \{(0,1),(0,-1),(1,0),(-1,0),(-1,-1),(-1,1),(1,-1),(1,1)\}. \tag{4-15}$$

We simulate this model with the two neighborhoods and the results are shown in the next section. Parameters used in the simulation are artificial parameters.

4.6 The Simulation of SIS-CA model

The spread of an SIS-type disease in a CA can be very complicated. Typically, the behavior of an SIS model can be very sensitive to values of the parameters and the time steps [6, 7, 15, 16]. We will see that this sensitivity also occurs in the SIS-CA model.

The lattice *L* in this simulation is the same size as section 4.3. The gray scale is used to represent the state of infection: from black color for state 0 (all people in the cell are not infected) to white color for state 1 (all people in the cell are infected). The infection starts from the middle cell, namely $(25,25)$ with the start state at $s_{25,25}^{0} = (0.7, 0.3)$. We assume that the connection factor for every cell $c_{kl}^{(i,j)} = 1$, the movement factor for every cell $m_{kl}^{(i,j)} = 0.5$, and the population *N* in each cell is equal to 100.

We show the behavior of the simulations for the following sets of parameters: $(\alpha,\beta)=\{(0.35,0.4),\ (0.6,0.4),\ (0.8,0.4)\}$, where α is the infection rate and β is the recovery rate. For each set of parameters we first show the results for the von Neumann and Moore neighborhoods for the time-development of the CA for times $t=0,20,40$. We then show the time dependence of the populations in the start cell (25,25), a non-start cell (25,35) on the vertical axis, and a non-start cell (35,35) on a diagonal from the start cell.

The time development of the CA for the von Neumann and Moore neighborhoods for parameter values $(\alpha,\beta)=(0.35,0.4)$ are shown in FIGURE (4-12). For both neighborhoods, the patterns are a uniform grey showing that all cells in the CA have similar *S* and *I* populations. The time development of the populations in selected cells will be shown below. In this case, the main difference between the two neighborhoods is that the disease spreads faster with the Moore neighborhood because each cell has 8 neighboring cells compared with 4 neighboring cells with the von Neumann neighborhood.

The time development of the CA for the two neighborhoods for parameter values $(\alpha,\beta)=(0.6,0.4)$ are shown in FIGURE (4-13). For these values, the behavior for the von Neumann and Moore neighborhoods are different. The von Neumann pattern remains a uniform grey pattern showing that all cells have similar *S* and *I* populations. However, the Moore neighborhood now shows a complicated pattern indicating that the *S* and *I* populations in neighboring cells can be very different.

The time development of the CA for the two neighborhoods for parameter values $(\alpha,\beta)=(0.8,0.4)$ are shown in FIGURE (4-14). In this case, both the von Neumann and Moore neighborhoods show complicated patterns of disease transmission.

von Neumann with $\alpha = 0.35$ and $\beta = 0.4$

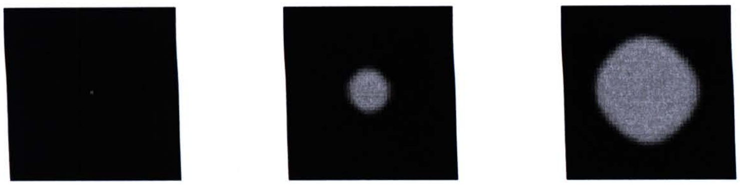

t = 0　　t = 20　　t = 40

Moore with $\alpha = 0.35$ and $\beta = 0.4$

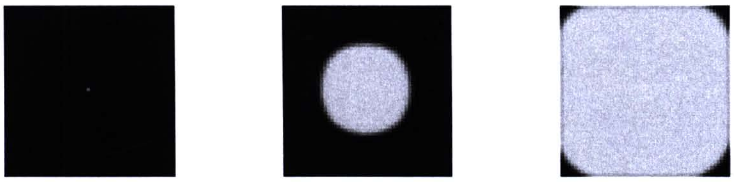

t = 0　　t = 20　　t = 40

FIGURE 4-12 SIS disease development patterns for von Neumann and Moore neighborhoods for (α, β)=(0.35,0.4)

von Neumann with $\alpha = 0.6$ and $\beta = 0.4$

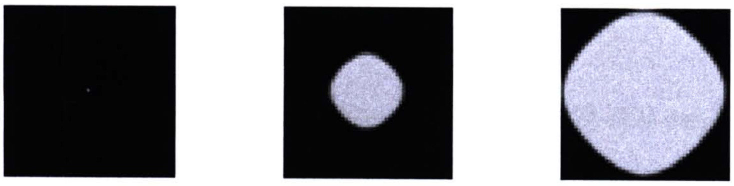

t = 0　　t = 20　　t = 40

Moore with $\alpha = 0.6$ and $\beta = 0.4$

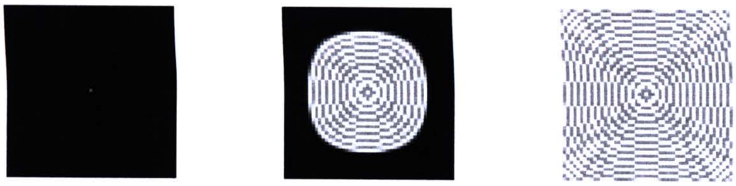

t = 0　　t = 20　　t = 40

FIGURE 4-13 SIS disease development patterns for von Neumann and Moore neighborhoods for (α, β)=(0.6,0.4)

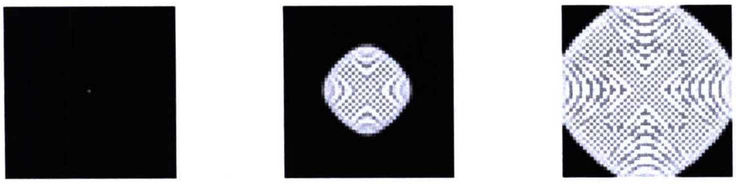

von Neumann with $\alpha = 0.8$ and $\beta = 0.4$

t = 0 t = 20 t = 40

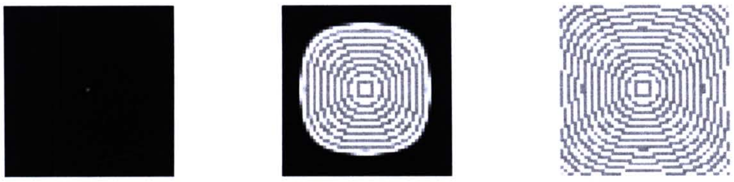

Moore with $\alpha = 0.8$ and $\beta = 0.4$

t = 0 t = 20 t = 40

FIGURE 4-14 SIS disease development patterns for von Neumann and Moore neighborhoods for (α, β)=(0.8,0.4)

We will now examine the disease patterns for 3 individual cells, a start cell (25,25), a non-start cell (25,35) on the vertical axis and a non-start cell (35,35) on a diagonal from the start cell.

FIGURE (4-15) shows the patterns for $(\alpha, \beta) = (0.35, 0.4)$ It can be seen that for both neighborhoods, all cells converge to a steady-state solution. For the Moore neighborhood, the *I* populations are greater than for the von Neumann and the steady state occurs faster. The patterns in the figure correspond to the uniform grey patterns shown in FIGURE (4-12).

FIGURE (4-16) shows the patterns for $(\alpha, \beta) = (0.6, 0.4)$. It can be seen that the behavior for the two neighborhoods is very different. For the von Neumann neighborhood the disease populations converge to a steady-state solution as in FIGURE (4-15). For the Moore neighborhood, the disease populations show a 2-point limit cycle behavior. The complicated patterns in FIGURE (4-13) occur because the limit cycle maxima and minima occur at different times in different cells.

FIGURE (4-17) shows the patterns for $(\alpha, \beta) = (0.8, 0.4)$. It can be seen that the disease patterns for both neighborhoods now show the 2-point limit cycle behavior. The complicated patterns in FIGURE (4-14) are again due to the maxima and minima of the limit cycles occurring at different times in different cells.

Finally, we show the time development of the total disease populations for the complete lattice in FIGURE (4-18) for $(\alpha,\beta)=(0.35,0.4)$ and $(0.8,0.4)$ for von Neumann and Moore neighborhoods. It can be seen that the total disease populations converge to a steady-state solution, but with a very small variation occurring in the Moore neighborhood for $(\alpha,\beta)=(0.8,0.4)$. Similar results have been obtained for parameter values of $(\alpha,\beta)=(0.6,0.4)$.

von Neumann

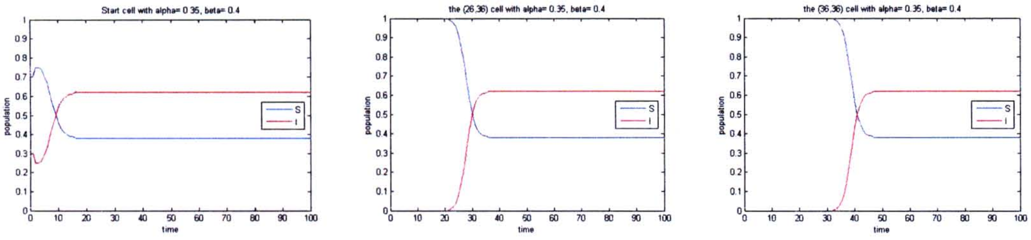

Start cell cell(25,35) cell(35,35)

Moore

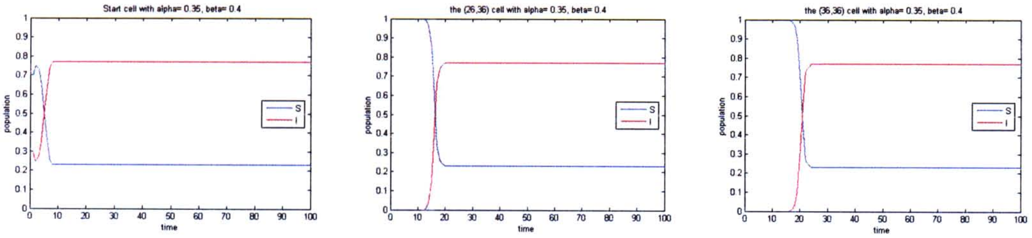

Start cell cell(25,35) cell(35,35)

FIGURE 4-15 Time development of *S* and *I* populations in the start cell and 2 non-start cells for (α,β)=(0.35,0.4).

von Neumann

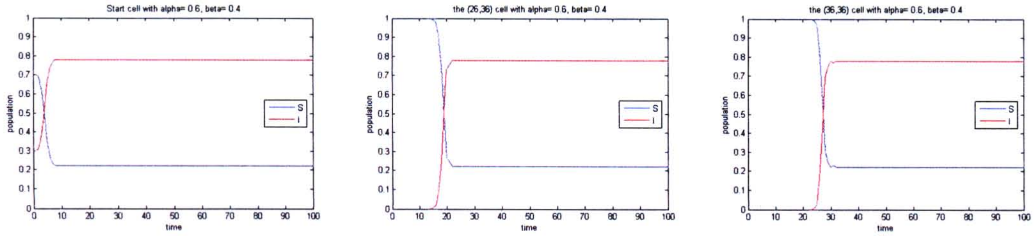

Start cell cell(25,35) cell(35,35)

Moore

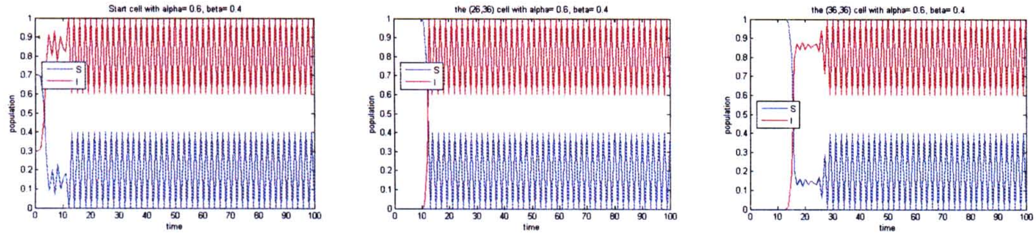

Start cell cell(25,35) cell(35,35)

FIGURE 4-16 Time development of *S* and *I* populations in the start cell and 2 non-start cells for (α,β)=(0.6,0.4).

von Neumann

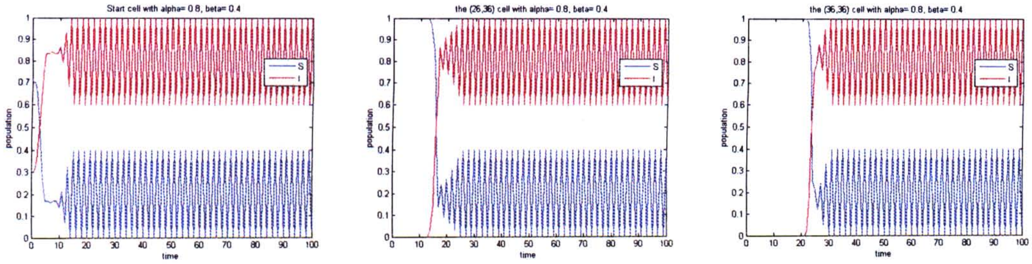

Start cell cell(25,35) cell(35,35)

Moore

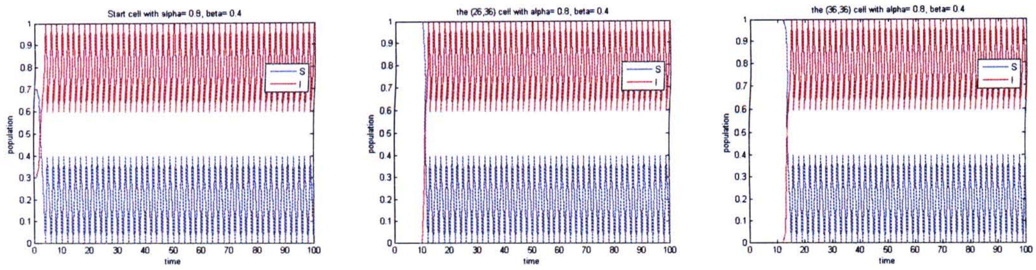

Start cell cell(25,35) cell(35,35)

FIGURE 4-17 Time development of *S* and *I* populations in the start cell and 2 non-start cells for (α,β)=(0.8,0.4).

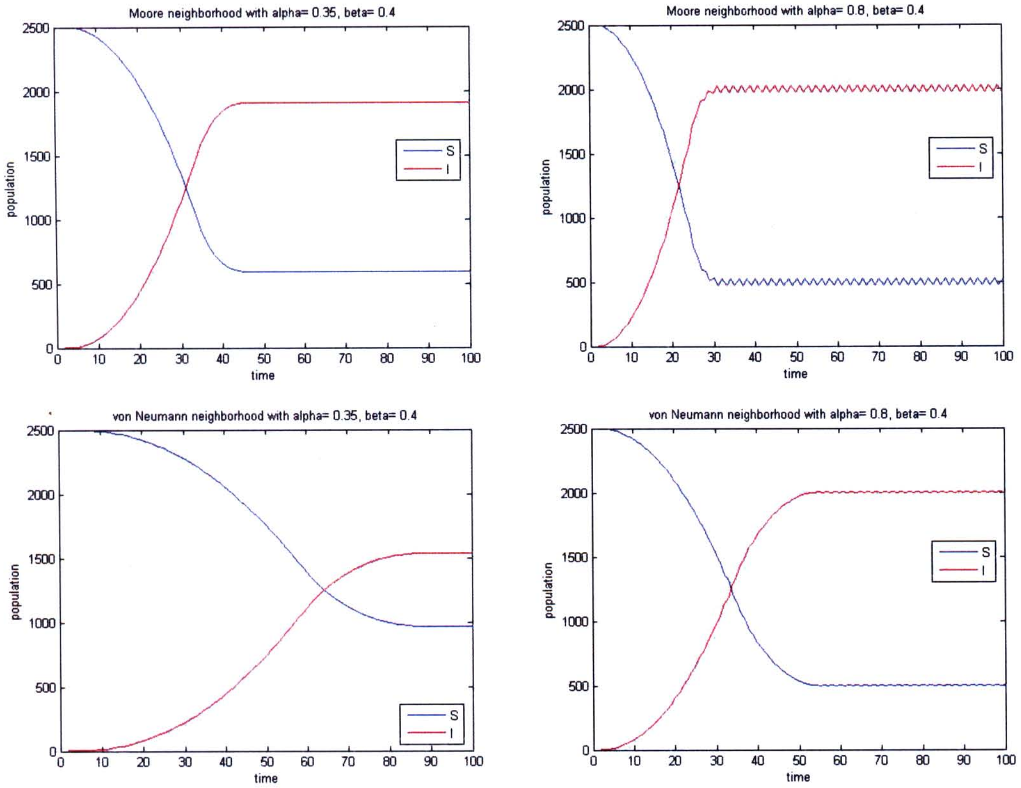

FIGURE 4-18 Time development of *S* and *I* populations for the complete lattice for (α, β)=(0.35,0.4) and (0.8,0.4).

From the discrete-time model for an SIS epidemic it is known that the qualitative behavior of the solution can be very sensitive to choice of parameter values and can show a bifurcation path to chaos [6, 7, 15, 16]. In particular, as the infection rate α is increased, the pattern goes from a steady-state solution to 2, 4, 8, etc. point limit cycles to chaos. The results shown above can be explained by noting that the effective infection rate is greater in a Moore neighborhood for the same value α than for a von Neumann neighborhood because of the larger number of neighbors.

A comparison of the results for the three sets of parameter values shows that the behavior of the *S* and *I* populations in individual cells can change significantly when parameter values are changed. However, the behavior of the populations in the whole lattice show only a small change and for all sets of parameters converge reasonably smoothly to equilibrium values for both Moore and von Neumann neighborhoods.